ISSN 1007-9327 (print)
ISSN 2219-2840 (online)

World Journal of *Gastroenterology*

World J Gastroenterol 2019 June 7; 25(21): 2539-2698

Published by Baishideng Publishing Group Inc

World Journal of Gastroenterology

Contents

Weekly Volume 25 Number 21 June 7, 2019

Contents

World Journal of Gastroenterology

Volume 25 Number 21 June 7, 2019

ABOUT COVER

Editorial board member of *World Journal of Gastroenterology*, Khaled Ali Jadallah, MD, Associate Professor, Doctor, Department of Internal Medicine, King Abdullah University Hospital, Jordan University of Science and Technology, Irbid 22110, Jordan

AIMS AND SCOPE

World Journal of Gastroenterology (*World J Gastroenterol*, *WJG*, print ISSN 1007-9327, online ISSN 2219-2840, DOI: 10.3748) is a peer-reviewed open access journal. The *WJG* Editorial Board consists of 642 experts in gastroenterology and hepatology from 59 countries.

The primary task of *WJG* is to rapidly publish high-quality original articles, reviews, and commentaries in the fields of gastroenterology, hepatology, gastrointestinal endoscopy, gastrointestinal surgery, hepatobiliary surgery, gastrointestinal oncology, gastrointestinal radiation oncology, *etc*. The *WJG* is dedicated to become an influential and prestigious journal in gastroenterology and hepatology, to promote the development of above disciplines, and to improve the diagnostic and therapeutic skill and expertise of clinicians.

INDEXING/ABSTRACTING

The *WJG* is now indexed in Current Contents®/Clinical Medicine, Science Citation Index Expanded (also known as SciSearch®), Journal Citation Reports®, Index Medicus, MEDLINE, PubMed, PubMed Central, Scopus and Directory of Open Access Journals. The 2018 edition of Journal Citation Report® cites the 2017 impact factor for *WJG* as 3.300 (5-year impact factor: 3.387), ranking *WJG* as 35th among 80 journals in gastroenterology and hepatology (quartile in category Q2).

RESPONSIBLE EDITORS FOR THIS ISSUE

Responsible Electronic Editor: *Yu-Jie Ma* **Proofing Editorial Office Director:** *Ze-Mao Gong*

NAME OF JOURNAL
World Journal of Gastroenterology

ISSN
ISSN 1007-9327 (print) ISSN 2219-2840 (online)

LAUNCH DATE
October 1, 1995

FREQUENCY
Weekly

EDITORS-IN-CHIEF
Subrata Ghosh, Andrzej S Tarnawski

EDITORIAL BOARD MEMBERS
http://www.wjgnet.com/1007-9327/editorialboard.htm

EDITORIAL OFFICE
Ze-Mao Gong, Director

PUBLICATION DATE
June 7, 2019

INSTRUCTIONS TO AUTHORS
https://www.wjgnet.com/bpg/gerinfo/204

GUIDELINES FOR ETHICS DOCUMENTS
https://www.wjgnet.com/bpg/GerInfo/287

GUIDELINES FOR NON-NATIVE SPEAKERS OF ENGLISH
https://www.wjgnet.com/bpg/gerinfo/240

PUBLICATION MISCONDUCT
https://www.wjgnet.com/bpg/gerinfo/208

ARTICLE PROCESSING CHARGE
https://www.wjgnet.com/bpg/gerinfo/242

STEPS FOR SUBMITTING MANUSCRIPTS
https://www.wjgnet.com/bpg/GerInfo/239

ONLINE SUBMISSION
https://www.f6publishing.com

World Journal of Gastroenterology

Submit a Manuscript: https://www.f6publishing.com

World J Gastroenterol 2019 June 7; 25(21): 2636-2649

DOI: 10.3748/wjg.v25.i21.2636

ISSN 1007-9327 (print) ISSN 2219-2840 (online)

ORIGINAL ARTICLE

Case Control Study

Gadoxetic acid-enhanced magnetic resonance imaging can predict the pathologic stage of solitary hepatocellular carcinoma

Yi-Chen Chou, I-Ha Lao, Pei-Ling Hsieh, Ying-Ying Su, Chee-Wai Mak, Ding-Ping Sun, Ming-Jen Sheu, Hsing-Tao Kuo, Tzu-Ju Chen, Chung-Han Ho, Yu-Ting Kuo

ORCID number: Yi-Chen Chou (0000-0002-2630-9773); I-Ha Lao (0000-0002-2935-8124); Pei-Ling Hsieh (0000-0001-8339-6140); Ying-Ying Su (0000-0002-3222-9163); Chee-Wai Mak (0000-0002-9814-0997); Ding-Ping Sun (0000-0001-9635-3254); Ming-Jen Sheu (0000-0001-9999-3222); Hsing-Tao Kuo (0000-0002-5841-974X); Tzu-Ju Chen (0000-0001-7840-9808); Chung-Han Ho (0000-0001-5925-8477); Yu-Ting Kuo (0000-0002-8704-0739).

Author contributions: All authors participated in the research. Kuo YT obtained funding, designed methodology, supervised the research, and wrote the article. Chou YC conducted investigations and wrote the original draft. Lao IH, Hsieh PL, Su YY, May CW, Sun DP, Sheu MJ, Kuo HT, and Chen TJ contributed to clinical survey and input of research methodology. Ho CH performed data curation and statistical analysis.

Institutional review board statement: This study was reviewed and approved by the Ethics Committee of Chi Mei Medical Center, Taiwan. IRB Serial No. 10702-007.

Informed consent statement: The need for informed consent was waived by the Institutional Review Board of Chi Mei Medical Center, Taiwan because of the retrospective nature of the study.

Conflict-of-interest statement: All authors declare no conflicts-of-interest related to this article.

Yi-Chen Chou, I-Ha Lao, Pei-Ling Hsieh, Ying-Ying Su, Chee-Wai Mak, Department of Medical Imaging, Chi Mei Medical Center, Tainan 710, Taiwan

I-Ha Lao, Biomedical Sciences, National Sun Yat-sen University, Kaohsiung 804, Taiwan

I-Ha Lao, School of Medicine, College of Medicine, Kaohsiung Medical University, Kaohsiung 807, Taiwan

Ding-Ping Sun, Department of Surgery, Chi Mei Medical Center, Tainan 710, Taiwan

Ding-Ping Sun, Department of Food Science and Technology, Chia Nan University of Pharmacy and Science, Tainan 717, Taiwan

Ming-Jen Sheu, Hsing-Tao Kuo, Division of Gastroenterology and Hepatology, Department of Internal Medicine, Chi Mei Medical Center, Tainan 710, Taiwan

Ming-Jen Sheu, Department of Medicinal Chemistry, Chia Nan University of Pharmacy and Science, Tainan 717, Taiwan

Hsing-Tao Kuo, Department of Senior Citizen Service Management, Chia Nan University of Pharmacy and Science, Tainan 717, Taiwan

Tzu-Ju Chen, Department of Pathology, Chi-Mei Medical Center, Tainan 710, Taiwan

Tzu-Ju Chen, Department of Optometry, Chung Hwa University of Medical Technology, Tainan 717, Taiwan

Tzu-Ju Chen, Institute of Biomedical Sciences, National Sun Yat-sen University, Kaohsiung 804, Taiwan

Chung-Han Ho, Department of Medical Research, Chi-Mei Medical Center, Tainan 710, Taiwan

Chung-Han Ho, Department of Hospital and Health Care Administration, Chia Nan University of Pharmacy and Science, Tainan 717, Taiwan

Yu-Ting Kuo, Department of Medical Imaging, Kaohsiung Medical University Hospital, Kaohsiung 807, Taiwan

Yu-Ting Kuo, Department of Radiology, Faculty of Medicine, College of Medicine, Kaohsiung Medical University, Kaohsiung 807, Taiwan

Corresponding author: Yu-Ting Kuo, MD, PhD, Doctor, Department of Medical Imaging, Chi Mei Medical Center, 901 Chung-Hwa Road, Yung-Kang District, Tainan 710, Taiwan.
y.kuo@mail.chimei.org.tw

Data sharing statement: No additional data are available.

STROBE statement: The manuscript was prepared according to the STROBE checklist.

Manuscript source: Unsolicited manuscript

Received: February 22, 2019
Peer-review started: February 22, 2019
First decision: March 27, 2019
Revised: April 30, 2019
Accepted: May 8, 2019
Article in press: May 8, 2019
Published online: June 7, 2019

P-Reviewer: Ding HG, Hashimoto N, Jia NY
S-Editor: Ma RY
L-Editor: Filipodia
E-Editor: Ma YJ

Telephone: +886-6-2812811

Abstract

BACKGROUND

Although important for determining long-term outcome, pathologic stage of hepatocellular carcinoma (HCC) is difficult to predict before surgery. Current state-of-the-art magnetic resonance imaging (MRI) using gadoxetic acid provides many imaging features that could potentially be used to classify single HCC as pT1 or pT2.

AIM

To determine which gadoxetic acid-enhanced MRI (EOB-MRI) findings predict pathologic stage T2 in patients with solitary HCC (cT1).

METHODS

Pre-operative EOB-MRI findings were reviewed in a retrospective cohort of patients with solitary HCC. The following imaging features were examined: Hyperintensity in unenhanced T2-weighted images, hypointensity in unenhanced T1-weighted images, arterial enhancement, corona enhancement, washout appearance, capsular appearance, hypointensity in the tumor tissue during the hepatobiliary (HB) phase, peritumoral hypointensity in the HB phase, hypointense rim in the HB phase, intratumoral fat, hyperintensity on diffusion-weighted imaging, hypointensity on apparent diffusion coefficient map, mosaic appearance, nodule-in-nodule appearance, and the margin (smooth or irregular). Surgical pathology was used as the reference method for tumor staging. Univariate and multivariate analyses were performed to identify predictors of microvascular invasion or satellite nodules.

RESULTS

There were 39 (34.2%; 39 of 114) and 75 (65.8%; 75 of 114) pathological stage T2 and T1 HCCs, respectively. Large tumor size (≥ 2.3 cm) and two MRI findings, *i.e.*, corona enhancement [odds ratio = 2.67; 95% confidence interval: 1.101-6.480] and peritumoral hypointensity in HB phase images (odds ratio = 2.203; 95% confidence interval: 0.961-5.049) were associated with high risk of pT2 HCC. The positive likelihood ratio was 6.25 (95% confidence interval: 1.788-21.845), and sensitivity of EOB-MRI for detecting pT2 HCC was 86.2% when two or three of these MRI features were present. Small tumor size and hypointense rim in the HB phase were regarded as benign features. Small HCCs with hypointense rim but not associated with aggressive features were mostly pT1 lesions (specificity, 100%).

CONCLUSION

Imaging features on EOB-MRI could potentially be used to predict the pathologic stage of solitary HCC (cT1) as pT1 or pT2.

Key words: Tumor invasiveness; Gadolinium ethoxybenzyl diethylenetriaminepentaacetic acid; Hepatobiliary; Contrast agent; Magnetic resonance imaging; Hepatocellular carcinoma

Core tip: Gadoxetic acid-enhanced-magnetic resonance imaging (EOB-MRI) has been shown to outperform other hepatocellular carcinoma (HCC) diagnostic tools. Our aim was to determine whether EOB-MRI findings could be used to predict pathologic stage T2 in patients with solitary HCC, clinical stage T1 (cT1). EOB-MRI was performed in 114 patients with solitary HCC [39 with pathologic stage T2 (pT2) and 75 with pT1]. Large tumor size, corona enhancement, and peritumoral hypointensity in hepatobiliary phase images were associated with high risk of pT2 HCC. The sensitivity of EOB-MRI for detecting pT2 HCC was 86.2% when two or three of these MRI features were present.

Citation: Chou YC, Lao IH, Hsieh PL, Su YY, Mak CW, Sun DP, Sheu MJ, Kuo HT, Chen

TJ, Ho CH, Kuo YT. Gadoxetic acid-enhanced magnetic resonance imaging can predict the pathologic stage of solitary hepatocellular carcinoma. *World J Gastroenterol* 2019; 25(21): 2636-2649
URL: https://www.wjgnet.com/1007-9327/full/v25/i21/2636.htm
DOI: https://dx.doi.org/10.3748/wjg.v25.i21.2636

INTRODUCTION

Hepatocellular carcinoma (HCC) is one of the most common malignancies worldwide, and its occurrence is highly related to hepatitis B and C virus infection. The TNM staging system of the American Joint Committee on Cancer seventh edition and Union for International Cancer Control defines T1 HCC as a solitary tumor without vascular invasion and defines T2 HCC as a solitary tumor with either gross or histologic involvement of vessels (microvascular or microscopic invasion)[1] or as multiple tumors (including satellite nodules), none more than 5 cm in greatest dimension. Therefore, clinical stage T1 (cT1) HCC on imaging studies can be either pathologic stage T1 or T2 (pT1 or pT2).

Methods of non-invasive prediction of pathologic stage of HCC, such as those using laboratory tests[2], have been investigated but not widely validated. Only a few imaging findings are widely accepted as prognostic biomarkers for HCC: tumor size, multifocal tumors, and vascular invasion[3-5]. The relative risk of HCC recurrence when patients present with macrovascular or microvascular invasion is 15- and 4.4-fold, respectively[6]. Patients with microvascular invasion or satellite nodules have higher rates of early and late recurrence and shorter overall survival after curative resection or liver transplantation[7-12]. Therefore, more extensive treatments, including wider surgical margin (if liver reserve is adequate) and more frequent follow-up examinations should be considered in such cases.

However, microvascular invasion and satellite nodules are difficult to detect preoperatively, even by current state-of-the-art imaging studies. Gadolinium ethoxybenzyl diethylene-triaminepentaacetic acid (Gd-EOB-DTPA) is a commercially available hepatocyte-specific magnetic resonance (MR) contrast agent that on intravenous administration can enhance the contrast of the liver parenchyma[13]. Gd-EOB-DTPA can be added to conventional dynamic MR imaging (MRI) for hepatobiliary (HB) phase imaging. EOB-MRI outperforms dynamic contrast-enhanced computed tomography and other MRI techniques as a tool for establishing a diagnosis of HCC[14-16]. Kim *et al*[17] reported that detection of more HCCs by EOB-MRI improved overall survival of patients initially evaluated by computed tomography. However, unlike conventional MRI, which uses extracellular contrast agents, EOB-MRI has some limitations, such as weaker arterial enhancement, a narrower window of peak arterial enhancement, and severe respiratory motion artifacts in some cases[18-21]. Moreover, the usefulness of EOB-MRI for predicting the presence of microvascular invasion or satellite nodules has not yet been well established.

The purpose of our study is to investigate whether the imaging features of solitary HCC on preoperative EOB-MRI can be used to predict pT2 HCC and whether the finding of more than one aggressive imaging feature could increase the reliability of this prediction.

MATERIALS AND METHODS

Study population

This single-center retrospective study was conducted from January 2012 to December 2017. We retrospectively reviewed records from the pathology database in our institute. In total, 376 patients with HCC received liver resection and had pT1 or pT2. The criteria for inclusion were: First, newly diagnosed solitary HCC on preoperative imaging without obvious vascular invasion, lymphadenopathy, or extrahepatic metastasis; second, a preoperative Gd-EOB-DTPA MRI study; and third, no other treatment besides surgery. We excluded patients with recurrent HCC (n = 31), with combined tumors (intrahepatic cholangiocarcinoma) (n = 5), with no preoperative EOB-MRI study (n = 69), with only a preoperative computed tomography imaging study (n = 104), with ruptured HCC and hemoperitoneum (n = 4), undertaking other preoperative treatments (radiofrequency ablation, transarterial chemoembolization, intra-arterial infusion chemotherapy, and stereotactic radiosurgery) (n = 10), with no

imaging study in our imaging archiving system (n = 1), with HCC on biopsy but only tumor necrosis postoperatively (n = 2), with two HCCs on EOB-MRI (clinical stage T2) (n = 28), and receiving segmentectomy limited to removal of only one tumor due to poor liver reserve (n = 8) (Figure 1).

Methods

We used Gd-EOB-DTPA (Primovist®, Bayer Healthcare, Berlin, Germany) as MRI contrast agent for these patients. Bolus injection of 10 mL of Gd-EOB-DTPA at the rate of 1 mL/s was immediately followed by a normal saline flush of 10-20 mL. In order to optimize hepatic arterial-phase timing, MRI was performed by using a 1.5-T system (Avanto, Siemens Healthineers, Erlangen, Germany) with 32 independent RF channels or another 1.5-T system (Aera, Siemens Healthineers) with 64 independent RF channels and body coils. A rectangular field of view of 32 cm × 24 cm to 29 cm × 22 cm was tailored for each patient.

The standard liver MRI protocol in our hospital consisted of a respiration-triggered fat-saturated T2-weighted fast spin-echo or turbo spin-echo sequence [repetition time (TR), 4175 ms; echo time (TE), 76 ms; acceleration factor, 2; number of excitation, 1; slice thickness, 5 mm], double-echo T1-weighted gradient-echo sequence (in-phase: TR, 164 ms; TE 4.76 ms; opposed-phase: TR, 164; TE 2.38 ms; acceleration factor, 2; number of excitation, 1; slice thickness, 5 mm), and a dynamic contrast-enhanced T1-weighted gradient-echo sequence with chemically selective fat suppression. The dynamic contrast-enhanced 3D MRI was performed using a volumetric interpolated breath-hold examination sequence (TR, 4.45 ms; TE, 1.60 ms; flip angle, 10° for arterial to transitional phase, 30° for HB phase; acceleration factor, 2; number of excitation, 1; slice thickness, 3 mm) with bolus-tracking protocol. Image acquisition began with the volumetric interpolated breath-hold examination sequence (arterial phase) and was initiated when the contrast medium was visible at the level of the celiac trunk of the abdominal aorta. We also acquired images of the portal venous phase at about 60-70 seconds, transitional phase at about 3 minutes, and HB phase at 20 min after the start of contrast medium injection. Diffusion-weighted imaging (with b values as 50, 400, and 800 s/mm^2) was performed using a respiratory-triggered single-shot echo-planar imaging sequence; then an apparent diffusion coefficient map was generated.

Characteristic MRI features

We measured the largest outer-edge-to-outer-edge dimension of the tumor including the capsule in the HB phase according to version 2017 of the Liver Imaging Reporting and Data System of the American College of Radiology[22]. The following imaging features were examined: hyperintensity in unenhanced T2-weighted images, hypointensity in unenhanced T1-weighted images, arterial enhancement, corona enhancement, washout appearance, capsular appearance, hypointensity in the tumor tissue during the HB phase, peritumoral hypointensity in the HB phase, hypointense rim in the HB phase, intratumoral fat, hyperintensity on diffusion-weighted imaging, hypointensity on apparent diffusion coefficient map, mosaic appearance, nodule-in-nodule appearance, and the margin (smooth or irregular)[3,14,23-29]. Corona enhancement was defined according to the Liver Imaging Reporting and Data System version 2017 as an uneven area of hyper-enhancement surrounding the hypervascular HCC in the late arterial phase or early portal venous phase. Peritumoral hypointensity in the HB phase was defined as irregular, wedge-shaped or a flame-like ring of enhancement surrounding the tumor and outside of the tumor margin usually with a lower intensity than liver parenchyma but a higher intensity than the tumor[27]. According to the Liver Imaging Reporting and Data System version 2017, the hypointense rim formed a discrete boundary between the tumor and its surroundings. Presence or absence of these findings in each individual set of images was recorded by two radiologists independently. Discrepancies were resolved by consensus.

Pathology evaluation

The pathology was analyzed by experienced pathologists after the surgery. The macroscopic and microscopic characteristics of the resected specimen included: Number and size of the HCC nodules, degree of histologic differentiation of HCC, status of microvascular invasion, presence or absence of satellite nodules, presence or absence of tumor necrosis, capsule formation with or without disruption, and stage of background liver parenchyma fibrosis. Microvascular invasion was identified on microscopic examination as tumor emboli in endothelial cell-lined vascular spaces. Satellite nodules were detected on microscopic examination as small HCCs separated from the main HCC by tumor-free liver parenchyma[8].

Statistical analysis

Continuous variables are presented as mean and standard deviation and were

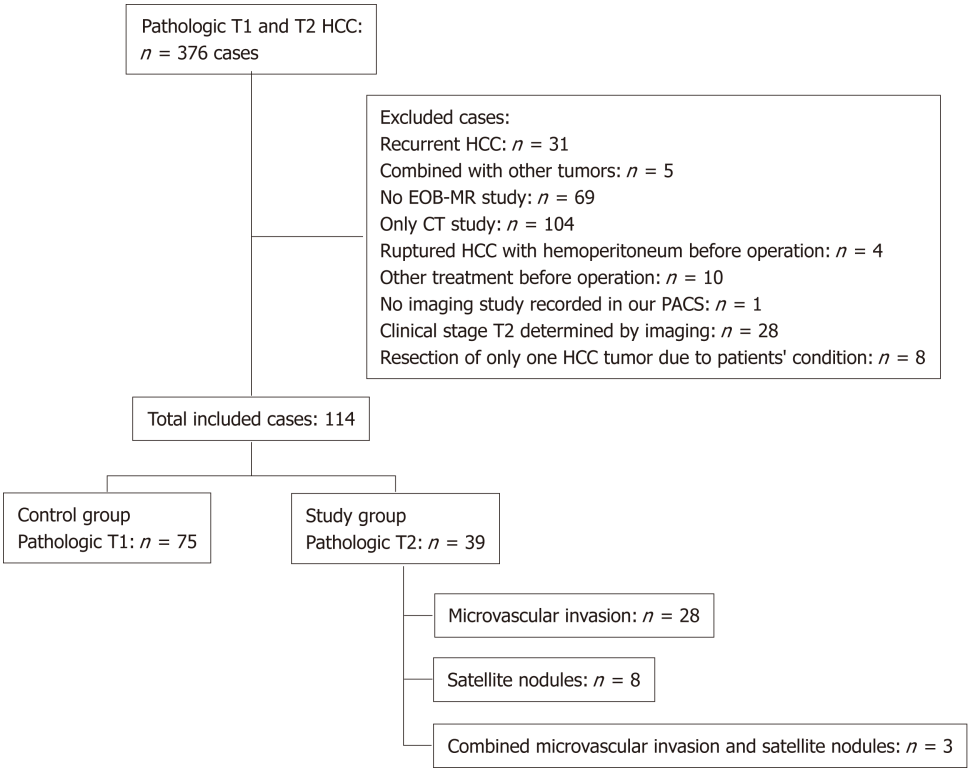

Figure 1 Flow chart of the study population selection process and the inclusion and exclusion criteria. HCC: Hepatocellular carcinoma; EOB-MRI: ethoxybenzyl magnetic resonance imaging; CT: Computed tomography.

analyzed statistically with the Student *t*-test. Categorical variables are presented as frequency and percentage and were analyzed with the Pearson chi-square test or Fisher exact test. The association (measured by odds ratio) of pathologic stage T2 HCC with all selected potential risk factors was assessed using univariate logistic regression analysis. In addition, the diagnostic accuracy of imaging findings for predicting pathologic stage T2 HCC was assessed using the ROC curve. SAS 9.4 for Windows (SAS Institute, Cary, NC, United States) and Prism 6 (GraphPad Software Inc., La Jolla, CA, United States) were used to perform these analyses. Statistical significance was considered as $P < 0.05$.

RESULTS

There was no significant difference in age, gender, hepatitis virus type, serum tumor biomarkers (alpha-fetoprotein and CA19-9), interval between imaging and surgery, and METAVIR score of liver fibrosis between the pT1 and pT2 groups (Table 1).

There were 114 patients included in our study (75 with pT1 HCC and 39 with pT2 HCC). In the pT2 group, 28 patients had a tumor with microvascular invasion, eight had a tumor with one or more satellite nodules, and three had a tumor with both microvascular invasion and one or more satellite nodules (Figure 1).

Regarding the imaging features, there was no significant between-group difference in T2 hyperintensity, T1 hypointensity, arterial enhancement, washout appearance, capsular appearance, hypointensity in the HB phase, intratumoral fat, hyperintensity on diffusion-weighted imaging, hypointensity on the apparent diffusion coefficient map, mosaic appearance, and the margin (smooth or irregular). Fourteen patients (35.9%) in the pT2 group and 13 patients (17.3%) in the pT1 group showed corona enhancement, with an odds ratio of 2.671 and 95% confidence interval (CI) of 1.101-6.480 ($P = 0.030$). HCCs with this imaging feature were more likely to be stage pT2. We also noted differing tendencies for peritumoral hypointensity to occur in the HB phase between the pT2 group ($n = 16$; 41.0%) and pT1 group ($n = 18$; 24%), with an odds ratio of 2.203 and 95%CI of 0.961-5.049 ($P = 0.062$), suggesting HCCs with this imaging feature also tend to be stage pT2 tumors (Tables 2 and 3) (Figures 2 and 3).

Three patients (7.7%) in the pT2 group and 24 patients (32%) in the pT1 had tumors smaller than or equal to 2 cm, with an odds ratio of 0.149 and 95%CI of 0.033-0.674 ($P = 0.013$). Tumors smaller or equal to 2 cm in diameter tended to be stage pT1. The

Table 1 Comparison of demographic and other characteristics between the pathologic stage T2 and T1 groups, *n* (%)

Characteristics	pT2, *n* = 39	pT1, *n* = 75	*P* value
Age, mean ± SD	60.54 ± 11.17	58.32 ± 10.95	0.3101
Gender			0.375
Male	26 (66.7)	57 (76.0)	
Female	13 (33.3)	18 (24.0)	
Hepatitis virus subtype			
HBV	21 (53.8)	50 (66.7)	0.223
HCV	15 (38.5)	21 (28.0)	0.292
HBV and HCV	3 (7.7)	3 (4.0)	0.385
Tumor marker			
AFP	415.3 ± 1536.1	812.3 ± 5922.0	0.5683
CA-19-9	116.2 ± 606.2	14.1 ± 15.6	0.2998
Interval between the dates of imaging and surgery, mean ± SD	17.69 ± 30.80	18.09 ± 20.58	0.9419
METAVIR score of liver fibrosis			0.7852
F0-F3	28 (71.79)	52 (69.33)	
F4	11 (28.21)	23 (30.67)	

HBV and HCV: Hepatitis viruses B and C; AFP: Alpha-fetoprotein; CA-19-9: Cancer antigen 19-9; pT1: Pathologic stage T1; pT2: Pathologic stage T2.

occurrence of another HB phase imaging feature, *i.e.*, the hypointense rim, differed between the pT2 group (n = 5, 12.8%) and pT1 group (n = 21, 28%), with an odds ratio of 0.378 and 95%CI of 0.130-1.098 (P = 0.074), indicating that HCC with this imaging feature tends to be stage pT1 (Tables 2 and 3) (Figures 4 and 5).

In our study using the Youden index, the optimal cut-point of tumor size was 2.3 cm. The area under the ROC curve (not shown) was 0.5745, which was not good enough for pT2 HCC prediction based only on tumor size. Other imaging findings suggesting pT2 in our study were corona enhancement and peritumoral hypointensity in the HB phase. Tumors had an odds ratio for being stage pT2 of 1.037 (95%CI: 0.285-3.766) in the presence of one aggressive feature (*i.e.*, tumor size larger than 2.3 cm in diameter, corona enhancement, or peritumoral hypointensity). The odds ratio further increased to 6.25 (95%CI 1.788-21.845) in the presence of two or three aggressive features. The sensitivity of EOB-MRI for detecting pT2 HCC was 86.2% (25/29) when the HCCs had two or three of these MRI features (Table 4).

Large HCCs (size ≥ 2.3 cm) tended to be pT2, but in the absence of corona enhancement or peritumoral hypointensity in the HB phase, a significant number of them were pT1. Large HCCs with a hypointense rim were less likely to be pT2 (odds ratio = 0.26; 95%CI: 0.0086-0.7810; P = 0.016) than large HCCs without this feature. Small HCCs (less than 2.3 cm) tended to be pT1 lesions, were likely to be pT2 in the presence of aggressive imaging features on EOB-MRI (odds ratio: 34.00; 95%CI: 3.251-355.6; P = 0.0006), and were pT1 in the presence of an HB phase hypointense rim. Large HCCs with aggressive imaging features and without hypointense rims were most likely to be pT2 lesions (Figure 6).

DISCUSSION

In our study, tumor size and the "aggressive" imaging features corona enhancement and peritumoral hypointensity tended to predict the pathologic stage of solitary HCC as pT2. However, tumor size alone was not a good predictor.

Tumor size is an important factor affecting the incidence of occult vascular invasion and advanced histologic grade in HCC. The incidence of microscopic vascular invasion increases with tumor size[5]. However, there is still no consensus about the best tumor cutoff size to predict microinvasion. The odds ratio for HCC with microvascular invasion was 7.1 (95%CI: 2.6-19.8) when preoperative tumor size was ≥ 5 cm in the study by Kaibori *et al*[30] and 3 (95%CI: 1.2-7.1) when tumor size was greater than 4 cm in the study by Esnaola *et al*[31]. In our study, the tumor cutoff size (measured on MRI) was 2.3 cm, which was close to that proposed by the American Joint Committee on Cancer[32,33].

Corona enhancement and peritumoral hypointensity were also considered as predictive factors of microvascular invasion in a study conducted by Miyata *et al*[34].

Table 2 Imaging characteristics compared between the pathologic stage T2 group and T1 group, *n* (%)

Characteristics	pT2, *n* = 39	pT1, *n* = 75	*P* value
T2 hyperintensity	37 (94.9)	68 (90.7)	0.716
T1 hypointensity	35 (89.7)	69 (92.0)	0.733
Arterial enhancement	38 (97.4)	70 (93.3)	0.662
Corona enhancement	14 (35.9)	13 (17.3)	0.037
Washout appearance	36 (92.3)	69 (92.0)	1.000
Capsular appearance	14 (35.9)	38 (50.7)	0.167
Hypointensity of tumor in the HB phase	37 (94.9)	74 (98.7)	0.269
Peritumoral hypointensity in the HB phase	16 (41.0)	18 (24.0)	0.084
Hypointense-rim in the HB phase	5 (12.8)	21 (28.0)	0.099
Intratumoral fat	8 (20.5)	18 (24.0)	0.815
Hyperintensity on DWI	39 (100.0)	72 (96.0)	0.550
Hypointensity on ADC map	16 (41.0)	32 (42.7)	1.000
Mosaic architecture	27 (69.2)	48 (64.0)	0.679
Margin type			0.503
Smooth	27 (69.2)	57 (76.0)	
Irregular	12 (30.8)	18 (24.0)	
AJCC v.7	39 (100.0)	75 (100.0)	
AJCC v.8			0.005
cT1a (≤ 2 cm)	3 (7.7)	24 (32.0)	
cT1b (> 2 cm)	36 (92.3)	51 (68.0)	

HB: Hepatobiliary; DWI: Diffusion weighted imaging; ADC: Apparent diffusion coefficient; AJCC: American Joint Committee on Cancer; pT1: Pathologic stage T1; pT2: Pathologic stage T2.

Satellite nodules were found to occur more commonly when HCC invades adjacent vessels[35,36]. Our results support these previous findings and are consistent with other previous studies showing greater micro-metastasis occurrence in areas of coronal enhancement[37,38].

The cause of peritumoral hypointensity on HB phase images is still not clear. One possibility is that tumor microinvasion into small portal branches results in hemodynamic and perfusion changes. Perfusion change may be associated with change in the levels of organic anion-transporting polypeptide and multidrug-resistant protein expressed on hepatocytes[27,39]. Our findings are consistent with the study conducted by Kim *et al*[27], which identified peritumoral hypointensity in the HB phase of EOB-MRI as a predictor of HCC microvascular invasion.

The imaging features with predictive value might also reflect tumor biology. Previous studies have shown that during hepatocarcinogenesis the arterial supply system gradually shifts from intranodular portal to intranodular arterial, and the venous drainage system shifts from hepatic venous to hepatic sinusoidal and then to portal venous[40]. These changes are observable on MRI studies. We found that regardless of size, tumors were more likely to be pT2 lesions when corona enhancement and peritumoral hypointensity are present in the HB phase. However, the relationship between these two features remains unclear. In our study, not all HCCs had both corona enhancement in the arterial/portal phase and peritumoral hypointensity in the HB phase. These features might reflect different stages of hepatocarcinogenesis. Further studies are mandatory to confirm this hypothesis. Nevertheless, identifying these imaging findings before treatment might have clinical implications, particularly because many HCCs can now be diagnosed based on typical imaging findings and be treated with local ablation techniques, such as radio-frequency ablation[41,42].

The hypointense rim in the HB phase was not only an ancillary feature favoring diagnosis of HCC over other malignancies in a previous study[22], but also a relatively "protective" imaging biomarker in our study. Even large HCCs with hypointense rim in the HB phase tended to be pT1 lesions (P = 0.0155). In our study, hypointense rim might also have had a protective effect in patients with a large HCC in the presence of aggressive imaging features. In previous studies, the prognosis of encapsulated HCC was considered to be better than that of more advanced HCC but worse than that of

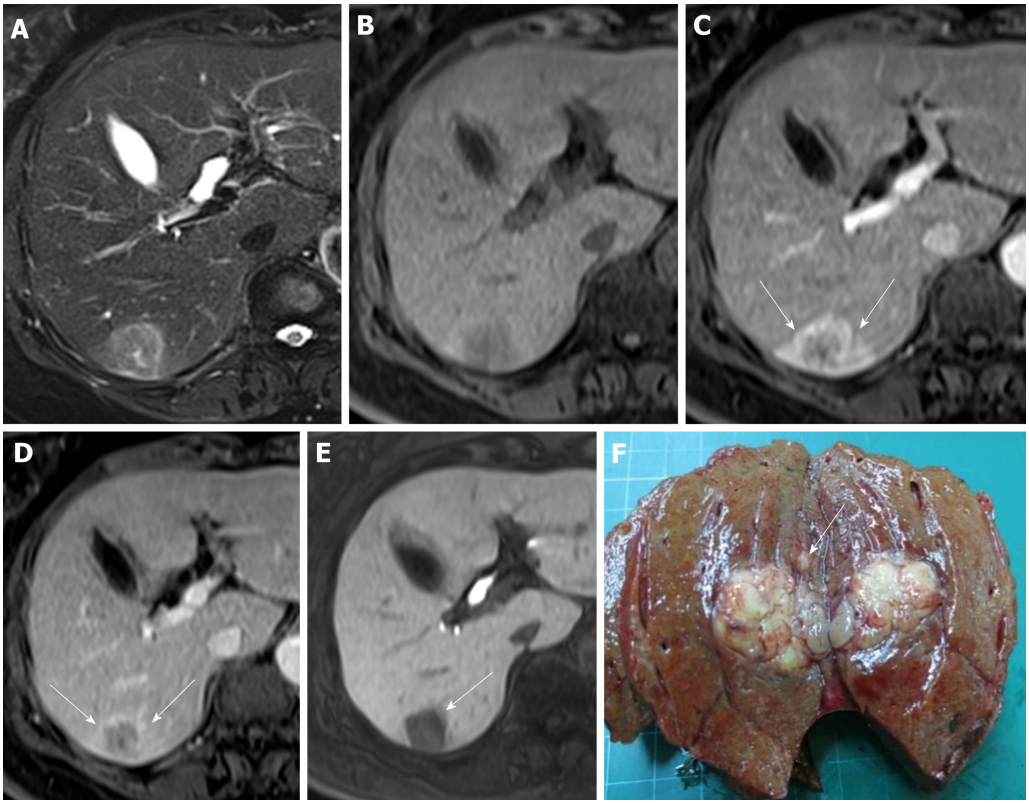

Figure 2 Images in a 73-year-old woman with a solitary hepatocellular carcinoma (tumor size 2.6 cm) in segment VI. A and B: Axial view of T2- and T1-weighted magnetic resonance images with fat suppression before administration of gadolinium ethoxybenzyl diethylene-triaminepentaacetic acid; C: Arterial phase and D: Portal venous phase showing hyperenhancing mass in segment VI with washout appearance, which is the typical appearance of hepatocellular carcinoma, as well as corona enhancement (arrow); E: Hepatobiliary phase, axial view of T1-weighted three-dimensional gradient-echo magnetic resonance image with fat suppression. The faint low signal intensity around the tumor is the peritumoral hypointensity (arrow); F: The tumor is identifiable postoperatively as a pT2 hepatocellular carcinoma because a satellite nodule surrounds the main tumor.

non-encapsulated HCC diagnosed at an earlier stage of hepatocellular carcinogenesis[43].

The tumor margin status of HCCs is controversial. Kim *et al*[44] concluded from univariate analysis but not multivariate analysis that non-smooth tumor margin is a risk factor for microvascular invasion. However, the odds ratio for smooth *versus* non-smooth tumor margin was not significantly different between the pT1 and pT2 groups in our study. Our findings are consistent with the results of Chandarana *et al*[45] who identified tumor multifocality on MRI and not tumor margin as the predictor of microvascular invasion.

A capsule or pseudocapsule is indicated by the presence of a "hypointense rim in the HB phase." However, one study concluded that the "capsule appearance" as indicated by HB phase hypointense rim could improve capsule detection[28]. This may explain why no significant difference in "capsule appearance" was found between the pT1 and pT2 groups in our study. In previous studies on HCCs, a better prognosis was indicated by the presence rather than the absence of a capsule[46,47]. Witjes *et al*[48] reported a greater frequency of microvascular invasion in those with enhanced capsular appearance on enhanced MR images than in those without it. This might also indicate a histological difference between the "capsule appearance" on dynamic contrast-enhanced MRI study and the presence of hypointense rim in the HB phase of EOB-MRI.

Limitations

Our study had some limitations. First, our study was a single-institute study with a relatively small sample size. Second, selection bias could not be avoided because of the retrospective nature of our study design. In it, the radiologists evaluating these features were blind to pathologic stage but not pathologic diagnosis. Prospective studies with larger population sizes should be performed to further validate our findings. Third, the time interval between MRI and surgery was about 18 d, and tumor progression during this interval may have confounded our correlation analysis between MRI and pathology. Fourth, because insurance reimbursement was an issue, we did not adjust contrast medium dose according to the body weight of each patient.

Table 3 The odds ratios for imaging features favoring a diagnosis of pathologic stage T2 over pT1

Features	Crude OR	95%CI	*P* value
T2 hyperintensity	1.904	(0.376-9.639)	0.436
T1 hypointensity	0.761	(0.201-2.874)	0.687
Arterial enhancement	2.714	(0.306-24.085)	0.370
Corona enhancement	2.671	(1.101-6.480)	0.030
Washout appearance	1.043	(0.246-4.419)	0.954
Capsular appearance	0.545	(0.246-1.208)	0.135
Hypointensity of tumor in the HB phase	0.250	(0.022-2.847)	0.264
Peritumoral hypointensity in HB phase	2.203	(0.961-5.049)	0.062
Hypointense-rim in the HB phase	0.378	(0.130-1.098)	0.074
Intratumoral fat	0.817	(0.319-2.093)	0.674
Mosaic architecture	1.266	(0.553-2.895)	0.577
Hyperintensity on DWI	N/A	N/A	N/A
Hypointensity ADC map	0.935	(0.426-2.050)	0.866
Tumor margin			
Smooth (baseline)			
Non-smooth	1.407	(0.594-3.333)	0.437
AJCC v.8			
cT1a (baseline)	1.00	Reference	
cT1b	6.727	(1.483-30.517)	0.014

Because all patients in the study group demonstrated hyperintensity on diffusion weighted imaging, we were not able to calculate the odds ratio and *P* value. HB: Hepatobiliary; DWI: Diffusion weighted imaging; ADC: Apparent diffusion coefficient; AJCC: American Joint Committee on Cancer; pT1: Pathologic stage T1; pT2: Pathologic stage T2; OR: Odds ratio; CI: Confidence interval.

This might affect the appearance of MR images. In addition, because prognosis was not assessed in this study, we did not determine whether these EOB-MRI imaging features could be used as biomarkers to predict clinical outcome.

CONCLUSION

Tumor size is an important prognostic factor, but in and of itself not good enough for classifying a single HCC lesion as pT1 or pT2 preoperatively. Imaging features of EOB-MRI might be useful to further stratify patients with solitary HCC. A large solitary HCC with corona enhancement and peritumoral hypointensity in the HB phase tends to be pT2, particularly in the absence of HB phase hypointense rim.

Table 4 Logistic regression estimates of odds ratios for pathologic stage T2 hepatocellular carcinoma in patients with solitary tumor on Gd-EOB-DTPA-enhanced magnetic resonance imaging

Combinations of aggressive features	Number of pT2 patients	OR (95%CI)
A = 0 and B = 0 and C = 0	4	Reference
Only A or Only B or Only C	10	1.037 (0.285-3.766)
A + B or B + C or A + C or A + B + C	25	6.250 (1.788-21.845)

Gd-EOB-DTPA: Gadolinium ethoxybenzyl diethylene-triaminepentaacetic acid; A = 0: Tumor size < 2.3 cm; B = 0: No peritumoral hypointensity on hepatobiliary phase; C = 0: No corona enhancement; A: Tumor size ≥ 2.3 cm; B: Presence of peritumoral hypointensity on hepatobiliary phase; C: Presence of corona enhancement; OR: Odds ratio; CI: Confidence interval.

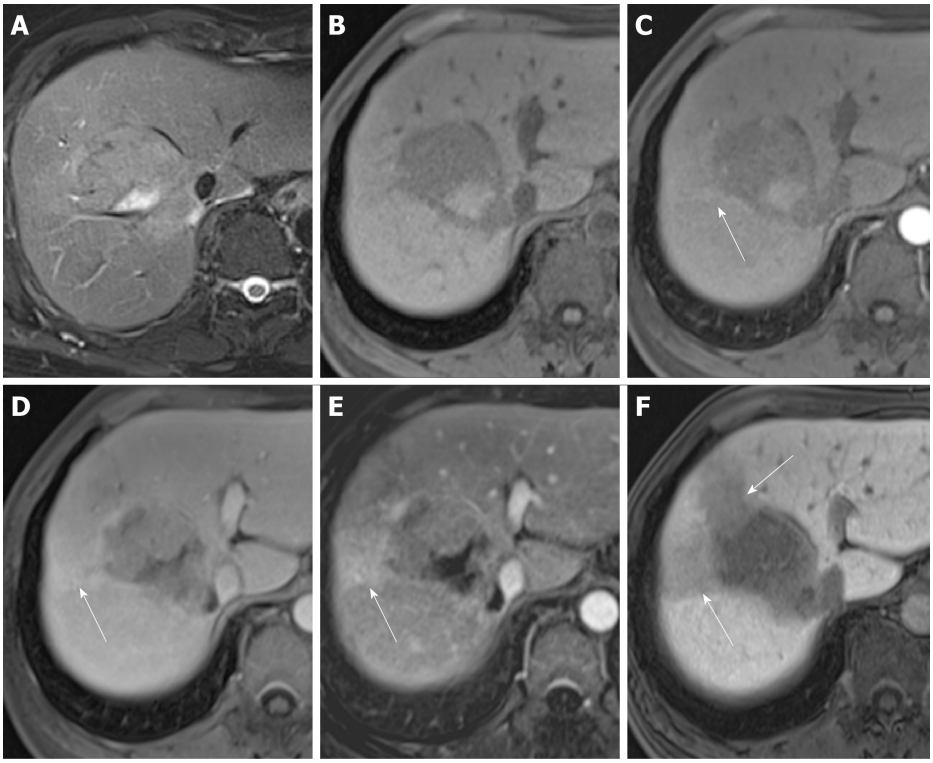

Figure 3 Images in a 64-year-old man with a solitary hepatocellular carcinoma (tumor size 5.5 cm) in segment VIII. A and B: Axial view of T2- and T1-weighted magnetic resonance images with fat suppression before administration of gadolinium ethoxybenzyl diethylene-triaminepentaacetic acid; C: Arterial phase and D: Portal venous phase showing hyperenhancing mass in segment VIII with partial washout appearance and corona enhancement (arrow); E: Subtracted images of the portal venous phase with more obvious corona enhancement; F: Hepatobiliary phase, T1-weighted three-dimensional gradient-echo magnetic resonance image (axial view) with fat suppression. The obvious flame-like peritumoral hypointensity (arrow) is noted. This tumor was identified postoperatively as a pT2 hepatocellular carcinoma owing to its microvascular invasion.

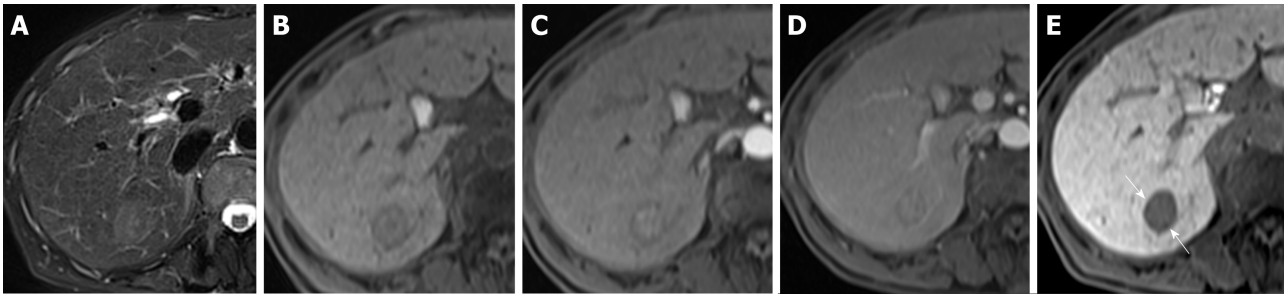

Figure 4 Images in a 65-year-old woman with a solitary hepatocellular carcinoma (tumor size 2.1 cm) in segment VII. A and B: Axial view of T2- and T1-weighted magnetic resonance images with fat suppression before administration of gadolinium ethoxybenzyl diethylene-triaminepentaacetic acid; C: Arterial phase showing hyperenhancing mass in segment VII; D: Portal venous phase with notable washout appearance of the hepatocellular carcinoma; E: Hepatobiliary phase, axial view of T1-weighted three-dimensional gradient-echo magnetic resonance image with fat suppression. The hypointense rim (arrow) is noted. Postoperatively, pT1 hepatocellular carcinoma was diagnosed.

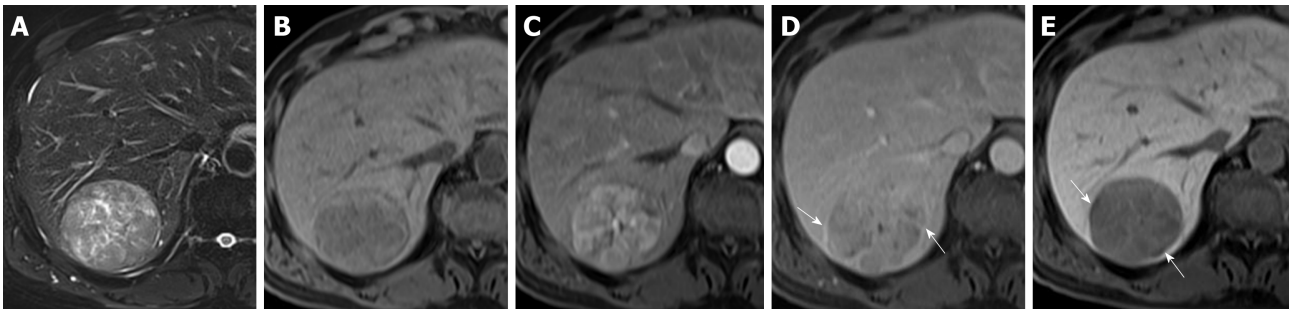

Figure 5 Images in a 60-year-old man with a solitary hepatocellular carcinoma (tumor size 5.5 cm) in segment VII. A and B: Axial view of T2- and T1-weighted magnetic resonance images with fat suppression before administration of gadolinium ethoxybenzyl diethylene-triaminepentaacetic acid; C: Arterial phase. Note the hyperenhancing hepatocellular carcinoma in segment VII; D: Portal venous phase. Note the capsular appearance (arrow) of the hepatocellular carcinoma; E: Hepatobiliary phase, axial view of T1-weighted three-dimensional gradient-echo magnetic resonance image with fat suppression. The tumor has an obvious hypointense rim (arrow). pT1 hepatocellular carcinoma was diagnosed postoperatively.

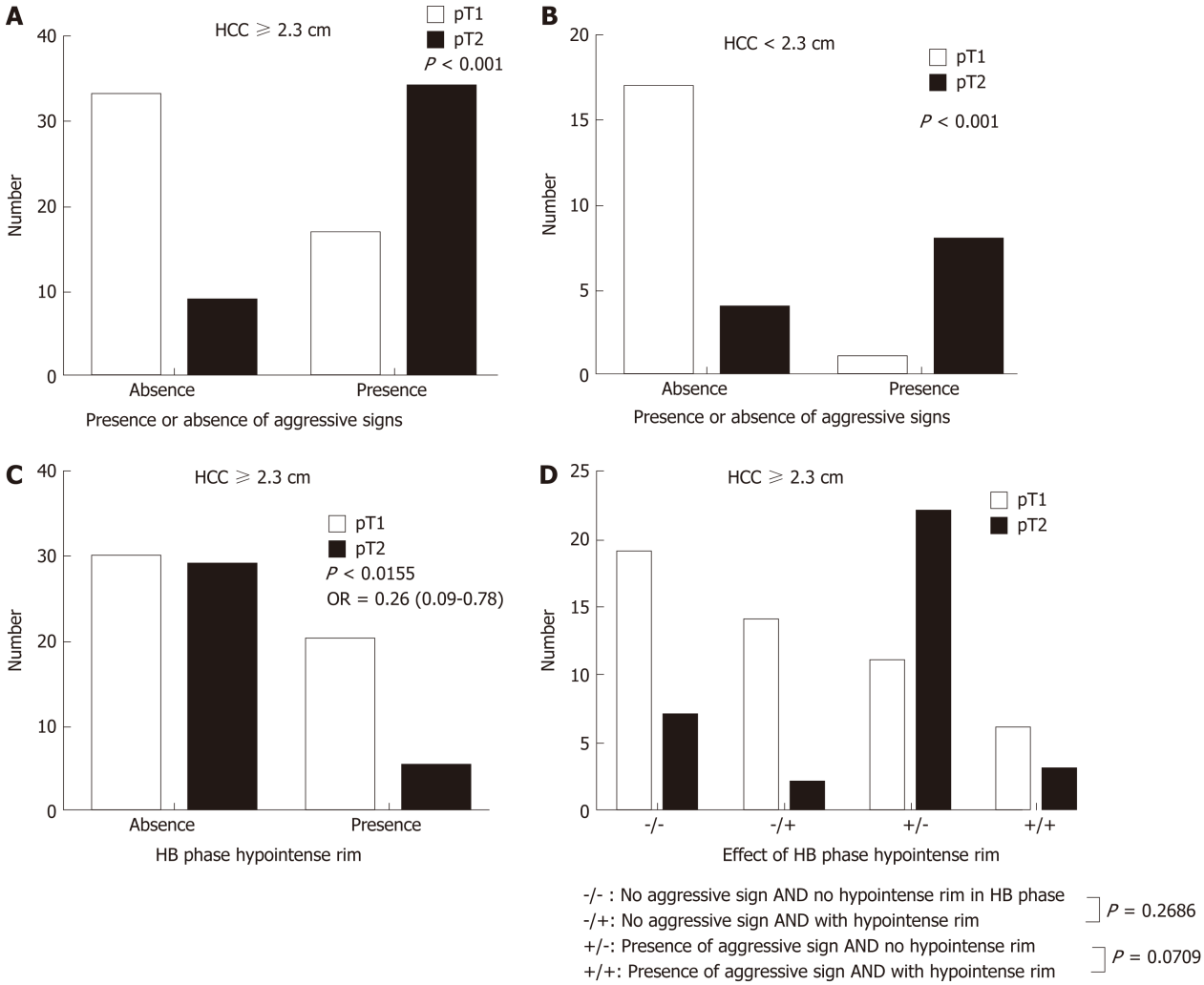

Figure 6 Solitary hepatocellular carcinomas on gadoxetic acid-enhanced magnetic resonance imaging. Large (≥ 2.3 cm) (A) and small (< 2.3 cm) (B) solitary hepatocellular carcinomas (HCCs) with aggressive imaging findings tend to be stage pT2 tumors ($P < 0.001$). Large (≥ 2.3 cm) HCCs with hypointense rims on MRI in the HB phase tend to be a stage pT1 tumors ($P = 0.0155$); C: Large HCCs with aggressive imaging features are more likely to be stage pT2 tumors if a hypointense rim is absent rather than present in the hepatobiliary phase; D: HCC: Hepatocellular carcinoma; HB: Hepatobiliary; pT1: Pathologic stage T1; pT2: Pathologic stage T2.

ARTICLE HIGHLIGHTS

Research background

Hepatocellular carcinoma (HCC) is one of the most common malignant tumors worldwide.

Higher pathologic stage of HCC has higher risk of recurrence and shorter survival. However, accurate prediction of pathologic stage from current pre-treatment imaging features is still difficult.

Research motivation
Modern magnetic resonance imaging (MRI) techniques using tissue-specific contrast agents provide many imaging features. We hypothesize that these imaging features may help to determine or predict pathologic stage of HCC.

Research objectives
To analyze the relationship between imaging features and the pathologic stage of HCC.

Research methods
There were 114 patients [75 with pathologic stage T1 (pT1) HCC and 39 with pathologic stage T2 (pT2) HCC] in this study. We reviewed each patient's imaging features on preoperative gadoxetic acid-enhanced (EOB) MRI. These included: hyperintensity in unenhanced T2-weighted images, hypointensity in unenhanced T1-weighted images, arterial enhancement, corona enhancement, washout appearance, capsular appearance, hypointensity in the tumor tissue during the hepatobiliary (HB) phase, peritumoral hypointensity in the HB phase, hypointense rim in the HB phase, intratumoral fat, hyperintensity on diffusion-weighted imaging, hypointensity on apparent diffusion coefficient map, mosaic appearance, nodule-in-nodule appearance, and the margin. All of these patients underwent surgery and sections of their tumor specimens were analyzed microscopically by an experienced pathologist. Univariate and multivariate analyses were performed to identify predictors of microvascular invasion or satellite nodules.

Research results
We found that large tumor size (≥ 2.3 cm) and two MR findings, *i.e.*, corona enhancement [odds ratio = 2.67; 95% confidence interval: 1.101-6.480) and peritumoral hypointensity in HB phase images (odds ratio = 2.203; 95% confidence interval: 0.961-5.049) were associated with high risk of pT2 HCC. The positive likelihood ratio was 6.25 (95% confidence interval: 1.788-21.845) and sensitivity of EOB-MRI for detecting pT2 HCC was 86.2% when two or three of these MRI features were present. Small tumor size and hypointense rim in the HB phase were regarded as benign features. Small HCCs with hypointense rim but not associated with aggressive features were mostly pT1 lesions (specificity, 100%).

Research conclusion
Imaging features on EOB-MRI could potentially be used to predict the pathologic stage of solitary HCC as pT1 or pT2.

Research perspectives
Imaging biomarkers of HCC are not yet well established. This study further identified imaging features of EOB-MRI that can be used to predict pathologic stage. This should be further validated in prospective studies. Research should be carried out to determine whether these MRI biomarkers help improve the clinical outcome of patients with HCC.

REFERENCES

1 **Roayaie S**, Blume IN, Thung SN, Guido M, Fiel MI, Hiotis S, Labow DM, Llovet JM, Schwartz ME. A system of classifying microvascular invasion to predict outcome after resection in patients with hepatocellular carcinoma. *Gastroenterology* 2009; **137**: 850-855 [PMID: 19524573 DOI: 10.1053/j.gastro.2009.06.003]

2 **Zhu Y**, Xu D, Zhang Z, Dong J, Zhou Y, Zhang WW, Hong L, Zhu WW. A new laboratory-based algorithm to predict microvascular invasion and survival in patients with hepatocellular carcinoma. *Int J Surg* 2018; **57**: 45-53 [PMID: 30075291 DOI: 10.1016/j.ijsu.2018.07.011]

3 **Khatri G**, Merrick L, Miller FH. MR imaging of hepatocellular carcinoma. *Magn Reson Imaging Clin N Am* 2010; **18**: 421-450, x [PMID: 21094448 DOI: 10.1016/j.mric.2010.08.002]

4 **Martins A**, Cortez-Pinto H, Marques-Vidal P, Mendes N, Silva S, Fatela N, Glória H, Marinho R, Távora I, Ramalho F, de Moura MC. Treatment and prognostic factors in patients with hepatocellular carcinoma. *Liver Int* 2006; **26**: 680-687 [PMID: 16842324 DOI: 10.1111/j.1478-3231.2006.001285.x]

5 **Pawlik TM**, Delman KA, Vauthey JN, Nagorney DM, Ng IO, Ikai I, Yamaoka Y, Belghiti J, Lauwers GY, Poon RT, Abdalla EK. Tumor size predicts vascular invasion and histologic grade: Implications for selection of surgical treatment for hepatocellular carcinoma. *Liver Transpl* 2005; **11**: 1086-1092 [PMID: 16123959 DOI: 10.1002/lt.20472]

6 **Iwatsuki S**, Dvorchik I, Marsh JW, Madariaga JR, Carr B, Fung JJ, Starzl TE. Liver transplantation for hepatocellular carcinoma: a proposal of a prognostic scoring system. *J Am Coll Surg* 2000; **191**: 389-394 [PMID: 11030244]

7 **Lim KC**, Chow PK, Allen JC, Chia GS, Lim M, Cheow PC, Chung AY, Ooi LL, Tan SB. Microvascular invasion is a better predictor of tumor recurrence and overall survival following surgical resection for hepatocellular carcinoma compared to the Milan criteria. *Ann Surg* 2011; **254**: 108-113 [PMID: 21527845 DOI: 10.1097/SLA.0b013e31821ad884]

8 **Plessier A**, Codes L, Consigny Y, Sommacale D, Dondero F, Cortes A, Degos F, Brillet PY, Vilgrain V, Paradis V, Belghiti J, Durand F. Underestimation of the influence of satellite nodules as a risk factor for post-transplantation recurrence in patients with small hepatocellular carcinoma. *Liver Transpl* 2004; **10**: S86-S90 [PMID: 14762846 DOI: 10.1002/lt.20039]

9 **Portolani N**, Coniglio A, Ghidoni S, Giovanelli M, Benetti A, Tiberio GA, Giulini SM. Early and late recurrence after liver resection for hepatocellular carcinoma: prognostic and therapeutic implications. *Ann Surg* 2006; **243**: 229-235 [PMID: 16432356 DOI: 10.1097/01.sla.0000197706.21803.a1]

10 **Sumie S**, Kuromatsu R, Okuda K, Ando E, Takata A, Fukushima N, Watanabe Y, Kojiro M, Sata M. Microvascular invasion in patients with hepatocellular carcinoma and its predictable clinicopathological factors. *Ann Surg Oncol* 2008; **15**: 1375-1382 [PMID: 18324443 DOI: 10.1245/s10434-008-9846-9]

11 **Vivarelli M**, Cucchetti A, Piscaglia F, La Barba G, Bolondi L, Cavallari A, Pinna AD. Analysis of risk factors for tumor recurrence after liver transplantation for hepatocellular carcinoma: key role of immunosuppression. *Liver Transpl* 2005; **11**: 497-503 [PMID: 15838913 DOI: 10.1002/lt.20391]

12 **Belghiti J**, Fuks D. Liver resection and transplantation in hepatocellular carcinoma. *Liver Cancer* 2012; **1**: 71-82 [PMID: 24159575 DOI: 10.1159/000342403]

13 **Seale MK**, Catalano OA, Saini S, Hahn PF, Sahani DV. Hepatobiliary-specific MR contrast agents: role in imaging the liver and biliary tree. *Radiographics* 2009; **29**: 1725-1748 [PMID: 19959518 DOI: 10.1148/rg.296095515]

14 **Ahn SS**, Kim MJ, Lim JS, Hong HS, Chung YE, Choi JY. Added value of gadoxetic acid-enhanced hepatobiliary phase MR imaging in the diagnosis of hepatocellular carcinoma. *Radiology* 2010; **255**: 459-466 [PMID: 20413759 DOI: 10.1148/radiol.10091388]

15 **Kim BR**, Lee JM, Lee DH, Yoon JH, Hur BY, Suh KS, Yi NJ, Lee KB, Han JK. Diagnostic Performance of Gadoxetic Acid-enhanced Liver MR Imaging versus Multidetector CT in the Detection of Dysplastic Nodules and Early Hepatocellular Carcinoma. *Radiology* 2017; **285**: 134-146 [PMID: 28609205 DOI: 10.1148/radiol.2017162080]

16 **Sano K**, Ichikawa T, Motosugi U, Sou H, Muhi AM, Matsuda M, Nakano M, Sakamoto M, Nakazawa T, Asakawa M, Fujii H, Kitamura T, Enomoto N, Araki T. Imaging study of early hepatocellular carcinoma: usefulness of gadoxetic acid-enhanced MR imaging. *Radiology* 2011; **261**: 834-844 [PMID: 21998047 DOI: 10.1148/radiol.11101840]

17 **Kim HD**, Lim YS, Han S, An J, Kim GA, Kim SY, Lee SJ, Won HJ, Byun JH. Evaluation of early-stage hepatocellular carcinoma by magnetic resonance imaging with gadoxetic acid detects additional lesions and increases overall survival. *Gastroenterology* 2015; **148**: 1371-1382 [PMID: 25733098 DOI: 10.1053/j.gastro.2015.02.051]

18 **Davenport MS**, Viglianti BL, Al-Hawary MM, Caoili EM, Kaza RK, Liu PS, Maturen KE, Chenevert TL, Hussain HK. Comparison of acute transient dyspnea after intravenous administration of gadoxetate disodium and gadobenate dimeglumine: effect on arterial phase image quality. *Radiology* 2013; **266**: 452-461 [PMID: 23192781 DOI: 10.1148/radiol.12120826]

19 **Huh J**, Kim SY, Yeh BM, Lee SS, Kim KW, Wu EH, Wang ZJ, Zhao LQ, Chang WC. Troubleshooting Arterial-Phase MR Images of Gadoxetate Disodium-Enhanced Liver. *Korean J Radiol* 2015; **16**: 1207-1215 [PMID: 26576109 DOI: 10.3348/kjr.2015.16.6.1207]

20 **Davenport MS**, Caoili EM, Kaza RK, Hussain HK. Matched within-patient cohort study of transient arterial phase respiratory motion-related artifact in MR imaging of the liver: gadoxetate disodium versus gadobenate dimeglumine. *Radiology* 2014; **272**: 123-131 [PMID: 24617733 DOI: 10.1148/radiol.14132269]

21 **Pietryga JA**, Burke LM, Marin D, Jaffe TA, Bashir MR. Respiratory motion artifact affecting hepatic arterial phase imaging with gadoxetate disodium: examination recovery with a multiple arterial phase acquisition. *Radiology* 2014; **271**: 426-434 [PMID: 24475864 DOI: 10.1148/radiol.13131988]

22 **National Cancer Institute**. The Liver Imaging Reporting and Data System version 2017. [Accessed 16 March 2018].American College of Radiology. Available from: URL: https://www.acr.org/Clinical-Resources/Reporting-and-Data-Systems/LI-RADS

23 **Kelekis NL**, Semelka RC, Worawattanakul S, de Lange EE, Ascher SM, Ahn IO, Reinhold C, Remer EM, Brown JJ, Bis KG, Woosley JT, Mitchell DG. Hepatocellular carcinoma in North America: a multiinstitutional study of appearance on T1-weighted, T2-weighted, and serial gadolinium-enhanced gradient-echo images. *AJR Am J Roentgenol* 1998; **170**: 1005-1013 [PMID: 9530051 DOI: 10.2214/ajr.170.4.9530051]

24 **Willatt JM**, Hussain HK, Adusumilli S, Marrero JA. MR Imaging of hepatocellular carcinoma in the cirrhotic liver: challenges and controversies. *Radiology* 2008; **247**: 311-330 [PMID: 18430871 DOI: 10.1148/radiol.2472061331]

25 **Ueda K**, Matsui O, Kawamori Y, Nakanuma Y, Kadoya M, Yoshikawa J, Gabata T, Nonomura A, Takashima T. Hypervascular hepatocellular carcinoma: evaluation of hemodynamics with dynamic CT during hepatic arteriography. *Radiology* 1998; **206**: 161-166 [PMID: 9423667 DOI: 10.1148/radiology.206.1.9423667]

26 **Ito K**, Fujita T, Shimizu A, Koike S, Sasaki K, Matsunaga N, Hibino S, Yuhara M. Multiarterial phase dynamic MRI of small early enhancing hepatic lesions in cirrhosis or chronic hepatitis: differentiating between hypervascular hepatocellular carcinomas and pseudolesions. *AJR Am J Roentgenol* 2004; **183**: 699-705 [PMID: 15333358 DOI: 10.2214/ajr.183.3.1830699]

27 **Kim KA**, Kim MJ, Jeon HM, Kim KS, Choi JS, Ahn SH, Cha SJ, Chung YE. Prediction of microvascular invasion of hepatocellular carcinoma: usefulness of peritumoral hypointensity seen on gadoxetate disodium-enhanced hepatobiliary phase images. *J Magn Reson Imaging* 2012; **35**: 629-634 [PMID: 22069244 DOI: 10.1002/jmri.22876]

28 **An C**, Rhee H, Han K, Choi JY, Park YN, Park MS, Kim MJ, Park S. Added value of smooth hypointense rim in the hepatobiliary phase of gadoxetic acid-enhanced MRI in identifying tumour capsule and diagnosing hepatocellular carcinoma. *Eur Radiol* 2017; **27**: 2610-2618 [PMID: 27770230 DOI: 10.1007/s00330-016-4634-6]

29 **Park MJ**, Kim YK, Lee MW, Lee WJ, Kim YS, Kim SH, Choi D, Rhim H. Small hepatocellular carcinomas: improved sensitivity by combining gadoxetic acid-enhanced and diffusion-weighted MR imaging patterns. *Radiology* 2012; **264**: 761-770 [PMID: 22843769 DOI: 10.1148/radiol.12112517]

30 **Kaibori M**, Ishizaki M, Matsui K, Kwon AH. Predictors of microvascular invasion before hepatectomy for hepatocellular carcinoma. *J Surg Oncol* 2010; **102**: 462-468 [PMID: 20872949 DOI: 10.1002/jso.21631]

31 **Esnaola NF**, Lauwers GY, Mirza NQ, Nagorney DM, Doherty D, Ikai I, Yamaoka Y, Regimbeau JM, Belghiti J, Curley SA, Ellis LM, Vauthey JN. Predictors of microvascular invasion in patients with hepatocellular carcinoma who are candidates for orthotopic liver transplantation. *J Gastrointest Surg* 2002; **6**: 224-32; discussion 232 [PMID: 11992808]

32 **Chun YS**, Pawlik TM, Vauthey JN. 8th Edition of the AJCC Cancer Staging Manual: Pancreas and

Hepatobiliary Cancers. *Ann Surg Oncol* 2018; **25**: 845-847 [PMID: 28752469 DOI: 10.1245/s10434-017-6025-x]

33 **Shindoh J**, Andreou A, Aloia TA, Zimmitti G, Lauwers GY, Laurent A, Nagorney DM, Belghiti J, Cherqui D, Poon RT, Kokudo N, Vauthey JN. Microvascular invasion does not predict long-term survival in hepatocellular carcinoma up to 2 cm: reappraisal of the staging system for solitary tumors. *Ann Surg Oncol* 2013; **20**: 1223-1229 [PMID: 23179993 DOI: 10.1245/s10434-012-2739-y]

34 **Miyata R**, Tanimoto A, Wakabayashi G, Shimazu M, Nakatsuka S, Mukai M, Kitajima M. Accuracy of preoperative prediction of microinvasion of portal vein in hepatocellular carcinoma using superparamagnetic iron oxide-enhanced magnetic resonance imaging and computed tomography during hepatic angiography. *J Gastroenterol* 2006; **41**: 987-995 [PMID: 17096068 DOI: 10.1007/s00535-006-1890-2]

35 **Okusaka T**, Okada S, Ueno H, Ikeda M, Shimada K, Yamamoto J, Kosuge T, Yamasaki S, Fukushima N, Sakamoto M. Satellite lesions in patients with small hepatocellular carcinoma with reference to clinicopathologic features. *Cancer* 2002; **95**: 1931-1937 [PMID: 12404287 DOI: 10.1002/cncr.10892]

36 **Choi JY**, Lee JM, Sirlin CB. CT and MR imaging diagnosis and staging of hepatocellular carcinoma: part II. Extracellular agents, hepatobiliary agents, and ancillary imaging features. *Radiology* 2014; **273**: 30-50 [PMID: 25247563 DOI: 10.1148/radiol.14132362]

37 **Sakon M**, Nagano H, Nakamori S, Dono K, Umeshita K, Murakami T, Nakamura H, Monden M. Intrahepatic recurrences of hepatocellular carcinoma after hepatectomy: analysis based on tumor hemodynamics. *Arch Surg* 2002; **137**: 94-99 [PMID: 11772225]

38 **Huang M**, Liao B, Xu P, Cai H, Huang K, Dong Z, Xu L, Peng Z, Luo Y, Zheng K, Peng B, Li ZP, Feng ST. Prediction of Microvascular Invasion in Hepatocellular Carcinoma: Preoperative Gd-EOB-DTPA-Dynamic Enhanced MRI and Histopathological Correlation. *Contrast Media Mol Imaging* 2018; **2018**: 9674565 [PMID: 29606926 DOI: 10.1155/2018/9674565]

39 **Kitao A**, Zen Y, Matsui O, Gabata T, Kobayashi S, Koda W, Kozaka K, Yoneda N, Yamashita T, Kaneko S, Nakanuma Y. Hepatocellular carcinoma: signal intensity at gadoxetic acid-enhanced MR Imaging--correlation with molecular transporters and histopathologic features. *Radiology* 2010; **256**: 817-826 [PMID: 20663969 DOI: 10.1148/radiol.10092214]

40 **Kitao A**, Zen Y, Matsui O, Gabata T, Nakanuma Y. Hepatocarcinogenesis: multistep changes of drainage vessels at CT during arterial portography and hepatic arteriography--radiologic-pathologic correlation. *Radiology* 2009; **252**: 605-614 [PMID: 19703890 DOI: 10.1148/radiol.2522081414]

41 **Takahashi S**, Kudo M, Chung H, Inoue T, Ishikawa E, Kitai S, Tatsumi C, Ueda T, Minami Y, Ueshima K, Haji S. Initial treatment response is essential to improve survival in patients with hepatocellular carcinoma who underwent curative radiofrequency ablation therapy. *Oncology* 2007; **72** Suppl 1: 98-103 [PMID: 18087189 DOI: 10.1159/000111714]

42 **Minami Y**, Kudo M. Radiofrequency ablation of hepatocellular carcinoma: a literature review. *Int J Hepatol* 2011; **2011**: 104685 [PMID: 21994847 DOI: 10.4061/2011/104685]

43 **Iguchi T**, Aishima S, Sanefuji K, Fujita N, Sugimachi K, Gion T, Taketomi A, Shirabe K, Maehara Y, Tsuneyoshi M. Both fibrous capsule formation and extracapsular penetration are powerful predictors of poor survival in human hepatocellular carcinoma: a histological assessment of 365 patients in Japan. *Ann Surg Oncol* 2009; **16**: 2539-2546 [PMID: 19533247 DOI: 10.1245/s10434-009-0453-1]

44 **Kim H**, Park MS, Choi JY, Park YN, Kim MJ, Kim KS, Choi JS, Han KH, Kim E, Kim KW. Can microvessel invasion of hepatocellular carcinoma be predicted by pre-operative MRI? *Eur Radiol* 2009; **19**: 1744-1751 [PMID: 19247666 DOI: 10.1007/s00330-009-1331-8]

45 **Chandarana H**, Robinson E, Hajdu CH, Drozhinin L, Babb JS, Taouli B. Microvascular invasion in hepatocellular carcinoma: is it predictable with pretransplant MRI? *AJR Am J Roentgenol* 2011; **196**: 1083-1089 [PMID: 21512074 DOI: 10.2214/AJR.10.4720]

46 **Lai EC**, Ng IO, Ng MM, Lok AS, Tam PC, Fan ST, Choi TK, Wong J. Long-term results of resection for large hepatocellular carcinoma: a multivariate analysis of clinicopathological features. *Hepatology* 1990; **11**: 815-818 [PMID: 2161393]

47 **Ng IO**, Lai EC, Ng MM, Fan ST. Tumor encapsulation in hepatocellular carcinoma. A pathologic study of 189 cases. *Cancer* 1992; **70**: 45-49 [PMID: 1318778]

48 **Witjes CD**, Willemssen FE, Verheij J, van der Veer SJ, Hansen BE, Verhoef C, de Man RA, Ijzermans JN. Histological differentiation grade and microvascular invasion of hepatocellular carcinoma predicted by dynamic contrast-enhanced MRI. *J Magn Reson Imaging* 2012; **36**: 641-647 [PMID: 22532493 DOI: 10.1002/jmri.23681]

Published By Baishideng Publishing Group Inc
7041 Koll Center Parkway, Suite 160, Pleasanton, CA 94566, USA
Telephone: +1-925-2238242
Fax: +1-925-2238243
E-mail: bpgoffice@wjgnet.com
Help Desk:http://www.f6publishing.com/helpdesk
http://www.wjgnet.com